Chinese Chemical Letters 32 (2021) 703–707

Contents lists available at ScienceDirect

Chinese Chemical Letters

journal homepage: www.elsevier.com/locate/cclet

Communication

Alkoxy encapsulation of carbazole-based thermally activated delayed fluorescent dendrimers for highly efficient solution-processed organic light-emitting diodes

Zhihua Ma[a], Yuchun Wan[a], Wenyue Dong[a], Zhenjun Si[a,*], Qian Duan[a], Shiyang Shao[b,*]

[a] School of Materials Science and Engineering, Changchun University of Science and Technology, Changchun 130022, China
[b] State Key Laboratory of Polymer Physics and Chemistry, Changchun Institute of Applied Chemistry, Chinese Academy of Sciences, Changchun 130022, China

ARTICLE INFO

Article history:
Received 3 May 2020
Received in revised form 28 May 2020
Accepted 19 June 2020
Available online 20 June 2020

Keywords:
Alkoxy encapsulation
Thermally activated delayed fluorescence
Dendrimer
Organic light-emitting diodes

ABSTRACT

Two *n*-butoxy-encapsulated dendritic thermally activated delayed fluorescent (TADF) emitters (namely **O-D1** and **O-D2**) with the first-/second-generation carbazoledendrons are designed and synthesized *via* C—N coupling between carbazoledendrons and 2,4,6-tris(4-bromophenyl)-1,3,5-triazine core. It is found that, compared with the commonly-used *tert*-butyl groups, the use of *n*-butoxy encapsulation groups can lead to smallersinglet-triplet energy gap for the dendrimers, producing stronger TADF effect together with faster reverse intersystem crossing process. Solution-processed TADF organic light-emitting diodes (OLEDs) utilizingalkoxy-encapsulated dendrimers **O-D1** and **O-D2** as emitters exhibitstate-of-the-art device efficiency withthe maximum external quantum efficiency up to 16.8% and 20.6%, respectively, which are ~1.6 and ~2.0 times that of the *tert*-butyl-encapsulated counterparts. These results suggest that alkoxy encapsulation of the carbazole-based TADF dendrimers can be a promising approach for developing highly efficient emitters for solution-processed OLEDs.

Thermally activated delayed fluorescence (TADF) materials have drawn increasing attention in recent years for their ability to utilize 100% excitons in organic light-emitting diodes (OLEDs) through the reverse intersystem crossing (RISC) process from triplet (T_1) to singlet (S_1) state enabled by small singlet-triplet energy gap (ΔE_{ST}) [1–5]. To date, most of the efficient TADF OLEDs are fabricated *via* vacuum-deposition technology [6–11]. While TADF materials suitable for solution processes that are cost-effective and compatible with large-area fabrication of devices are relatively scarce [12–30].

Dendritic luminescent materials, which feature branched structures and good solubility in organic solvents, are a kind of promising solution-processed materials for OLED applications [31]. Compared to polymeric materials which may suffer from wide molecular-weight distribution and terminal defects, the unique advantage of dendrimers is that they have absolute molecular weights and well-defined chemical structures. Moreover, the periphery-core structure of dendrimer can prevent concentration quenching of the emitting center, making them suitable for developing high-efficiency solution-processed OLEDs. However, up to now, although many fluorescent and phosphorescent dendrimers are developed [31,32], the categories of TADF dendrimers are relatively rare, and their device efficiency still needs to be improved [33–39]. Since Yamamoto *et al.* first reported the TADF dendrimers with electron-accepting triazine unit as the core and electron-donating 1st-4th generation carbazoledendrons as the periphery [33], several strategies have been demonstrated to improve the device efficiency of TADF dendrimers. For example, by introducing alkyl or aryl groups into carbazoledendrons to enhance the hydrophobicity for lamination of electron-transporting layers, external quantum efficiency (EQE) up to 9.4% is realized for the fully solution-processed OLEDs [34]. Yang *et al.* have reported carbazole-based dendrimers by using diphenyl ketone as the acceptors, exhibit promising EQE of 13.8% for the non-doped solution-processed OLEDs [36]. Recently, Jiang *et al.* have reported TADF dendrimers by using *N,N'*-dicarbazolyl-3,5-benzene (mCP) as the exciplex-forming dendrons, giving the high maximum EQE of 16.5% for solution-processed OLEDs with 4,6-bis(3,5-di(pyridin-3-yl)phenyl)-2-methylpyrimidine (B3PYMPM) as electron-transporting material [38]. Nevertheless, it is noted that highly efficient TADF dendrimers with internal quantum efficiency approaching 100% are still scarce. Design strategy for TADF dendrimers to further improve their device efficiency is still needed.

* Corresponding authors.
E-mail addresses: szj@cust.edu.cn (Z. Si), ssyang@ciac.ac.cn (S. Shao).

https://doi.org/10.1016/j.cclet.2020.06.025

Here we report a novel strategy for highly efficient TADF dendrimers by alkoxy encapsulation of the dendritic carbazole-based donor-acceptor emitters. The alkoxyl groups are expected to increase the electron-donating ability of carbazoledendron without significantly lowering the triplet state [40], and thus can reduce the energy of S_1 states while keeping the T_1 states, leading to smaller ΔE_{ST} and stronger TADF effect. Using this strategy, two dendrimers, namely **O-D1** and **O-D2** (Fig. 1), which contain the first-/second-generation carbazoledendrons bearing *n*-butoxyen capsulation groups as donor and triphenyltriazine as acceptor are designed and synthesized. It is found that, compared to the commonly-used *tert*-butyl groups, introduction of alkoxy encapsulating groups into the dendrimers can reduce the ΔE_{ST}, leading to stronger TADF effect together with faster RISC process. Consequently, solution-processed TADF OLEDs using the alkoxy-encapsulated dendrimers **O-D1** and **O-D2** exhibit state-of-the-art device efficiency with maximum external quantum efficiency of 16.8% and 20.6%, respectively, which are ~1.6 and ~2.0 folds that of the *tert*-butyl-encapsulated counterparts.

The chemical structures of the dendrimers are displayed in Fig. 1. The alkoxy-encapsulated dendrimers **O-D1** and **O-D2** contain the first-/second-generation carbazoledendrons bearing *n*-butoxyen capsulating groups as the donor and tripenyltriazine core as acceptor. For comparison, the alkyl-encapsulated dendrimer **C-D1** consisting of the first-generation carbazoledendron with *tert*-butyl terminal groups as donor and tripenyltriazine core as acceptor is also provided. All the dendrimers were facilely synthesized *via* the palladium-catalyzed C—N coupling of the carbazoledendrons with the 2,4,6-tris(4-bromophenyl)-1,3,5-triazine core in good yields (61%–80%) (Scheme S1 in Supportinginformation). Their chemical structures were confirmed by ^{1}H and ^{13}C NMR spectra, matrix-assisted laser desorption ionization time-of-flight (MALDI-TOF) mass spectrometry and elemental analysis (Figs. S1-S9 in Supporting informaiton). The three dendrimers possess excellent solubility in common solvents such as tetrahydrofuran, chloroform, toluene, chlorobenzene and so on, indicating they are suitable for fabrication of solution-processed OLEDs.

To get the insight into the electronic structure of the dendrimers, density functional theory (DFT) calculation was carried out to investigate their frontier orbital distributions. Meanwhile, the time dependent density functional theory (TD-DFT) analysis are also performed to explore the electron transition and excited energy levels of the lowest singlet and triplet states. As shown in Fig. 2, the highest occupied molecular orbital (HOMO) of the dendrimers are mainly distributed on the carbazoledendrons, while the lowest unoccupied molecular orbital (LUMO) are localized on the triphenyltriazine core. The calculated HOMO/LUMO levels are -5.25/-2.00 eV, -4.93/-1.92 eV and -4.73/-2.36 eV for **C-D1**, **O-D1** and **O-D2** respectively, which are in the same trend as the experimental values determined by cyclic voltammetry (Table 1 and Fig. S10 in Supporting information). The much higher HOMO level of **O-D1** than **C-D1** is attributed to the much stronger electron-donating ability of the *n*-butoxy groups than the *tert*-butyl ones, while the higher HOMO level of **O-D2** compared to **O-D1** can be assigned to the more dispersed HOMO distribution in the second-generation carbazoledendrons. The elevated HOMO levels for the *n*-butoxy-encapsulated dendrimers should be preferable for hole injection from the anode to the dendrimers. Moreover, owing to the separated HOMO and LUMO distributions, the dendrimers exhibit small ΔE_{ST} values, indicating their potential as TADF emitters. Importantly, it is found that on going from **C-D1** to **O-D1** and **O-D2**, the ΔE_{ST} value is gradually decreased from 0.30 eV to 0.23 eV and 0.03 eV, respectively. The lowered ΔE_{ST} of **O-D1** compared with **C-D1** indicates that the electron-rich *n*-butoxy group can lower the S_1 state (by 0.22 eV) to a greater extent than the T_1 state (by 0.15 eV). In addition, the lower ΔE_{ST} of **O-D2** than **O-D1** is also reasonable considering the more dispersed HOMO distribution along the second-generation carbazoledendrons which leads to smallerelectron cloud overlap between the donor and acceptor.

The absorption and photoluminescence (PL) spectra of the dendrimers are presented in Figs. 3a and b. All the dendrimers exhibit strong π-π^* transition bands below 320 nm in toluene, together with broad absoptions at 350−450 nm which mainly belong to the intramolecular charge transfer transition. The PL spectra of the dendrimers in toluene exhibit broad and unstructured emission bands with the peaks located at 444−509 nm attributed to thecharge transfer emission. Compared with **C-D1**, **O-D1** show red-shifted emission by 51 nm, in linewith the stronger electron-donating ability of the *n*-butoxy groups than that of *tert*-butyl ones. From **O-D1** to **O-D2**, the emissoin is further red-shifted by 14 nm because of the extended conjugation of the second-generation carbazole dendron. PL spectra of the dendrimers in neat film show similar charge transfer emission as in solution, with the emission peaks red-shifted in the trend of **C-D1** (452 nm), **O-D1** (515 nm) and **O-D2** (541 nm). PL spectra of the dendrimers in doped films (10 wt% in host material Ad-4D2 [41], whose chemical structure is shown in Fig. 4a), however, exhibit hypochromic shift for the emission bands relative to the neatfilms, indicating the weaker intermolecular interaction of the dendrimers in this case (Fig. S11 in Supporting information). To determine the T_1 state, phosphorescence spectra of the dendrimers are measured in

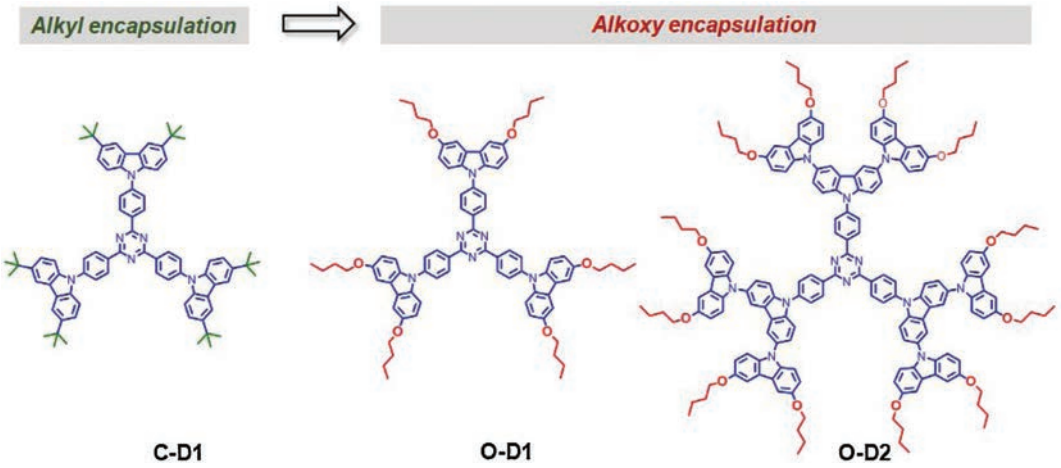

Fig. 1. Chemical structures of the alkoxy-encapsulated dendrimers and the alkyl-encapsulated control compound.

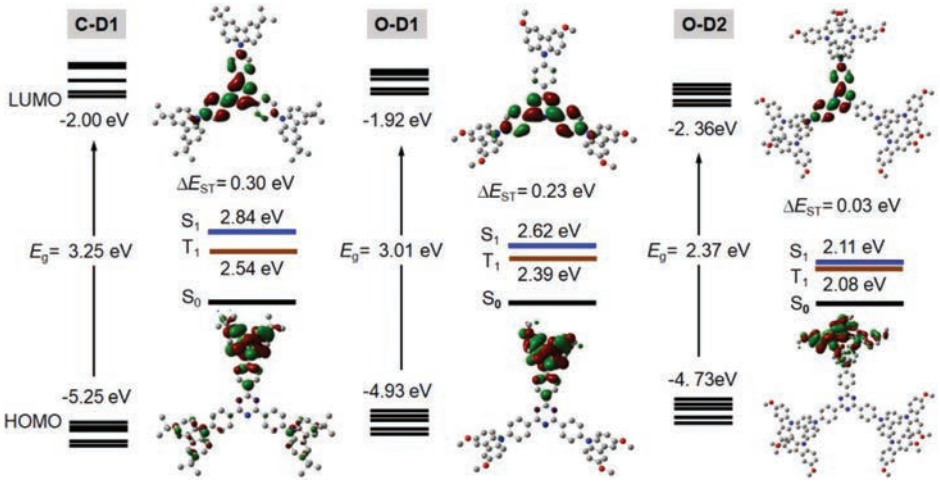

Fig. 2. HOMO/LUMO distributions and excited energy levels by (TD-)DFT calculation for the dendrimers at B3LYP/6-31 G(d) level. Methoxy groups are used instead of the *n*-butoxy ones in the calculation.

Table 1
Physical properties of the TADF dendrimers.

Dendrimer	λ_{abs}[a] (nm)	$\lambda_{PL,\ tol}$[b] (nm)	$\lambda_{PL,\ film}$[c] (nm)	λ_{Phos}[d] (nm)	PLQY[e] (%)	τ_p/τ_d[f] (μs)	HOMO/LUMO[g] (eV)	$S_1/T_1/\Delta E_{ST}$[h] (eV)
C-D1	296, 383	444	452	432	53	0.006/0.71	−5.58/−2.89	3.08/2.87/0.21
O-D1	311, 397	495	515	438	65	0.011/0.82	−5.29/−2.87	2.92/2.83/0.09
O-D2	305, 376, 410	509	541	442	74	0.017/1.43	−5.18/−2.94	2.83/2.81/0.02

[a] Absorption maxima.
[b] Emission peak in toluene (10^{-5} mol/L).
[c] Emission peak in neat film.
[d] Phosphorescent peak in toluene at 77 K.
[e] Photoluminescence quantum efficiency for doped films of 10 wt% dendrimers in Ad-4D2.
[f] Lifetimes for prompt (τ_p) and delayed component (τ_d).
[g] HOMO/LUMO levels calculated from oxidation/reduction potentials by CV characteristics.
[h] S_1 levels determined from onset of fluorescence spectra, T_1 levels from the highest energy peak of phosphorescent spectra and the S_1-T_1 energy splitting.

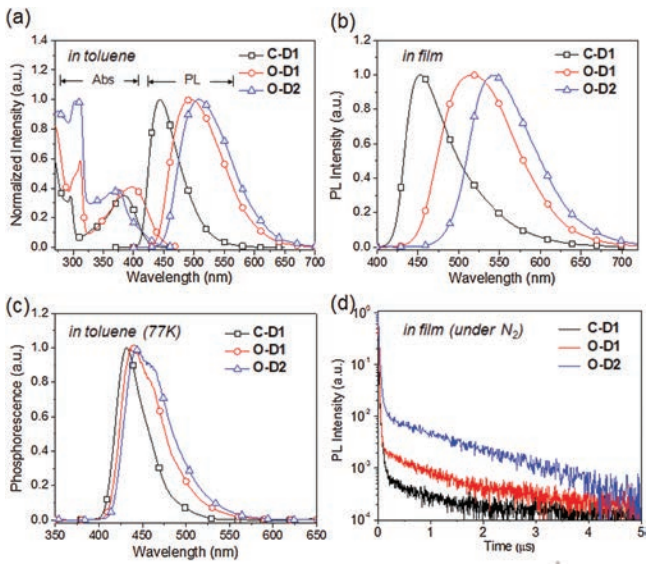

Fig. 3. Absorption (Abs) and PL spectra in toluene (10^{-5} mol/L) (a) and film state (b), phosphorescent spectra (in toluene, 77 K), (c) and the transient PL decay curves for films of the dendrimers in Ad-4D2 (10 wt%) under N_2 (d).

toluene at 77 K (Fig. 3c). The T_1 energy levels calculated from the highest peaks of the phosphorescence spectra are 2.87 eV, 2.83 eV and 2.81 eV for **C-D1**, **O-D1** and **O-D2**, respectively. Consequently, the experimental ΔE_{ST} values determined from the difference between S_1 and T_1 energy levels are 0.21 eV for **C-D1**, 0.09 eV for **O-D1** and 0.02 eV for **O-D2** (Table 1). Compared to **C-D1**, **O-D1** and **O-D2** exhibit much smaller ΔE_{ST} values, which is in consistence with the TD-DFT calculations. Such small ΔE_{ST} values make them promising TADF candidates. To confirm the TADF property, transient PL decay characteristics of the dendrimers are measured. As shown in Fig. 3d, all the dendrimers show decay curves consisting of a prompt component and a delayed component. The lifetimes of the delayed components (τ_d) are in the range of 0.71–1.43 μs, with the contribution of 12%, 33% and 64% for **C-D1**, **O-D1** and **O-D2**, respectively. The RISC rate constants (k_{RISC}) of the dendrimers are calculated to be 0.34×10^{-6} s^{-1}, 1.07×10^{-6} s^{-1} and 1.67×10^{-6} s^{-1} for **C-D1**, **O-D1** and **O-D2**, respectively, suggesting the favorable RISC processes from the T_1 state to S_1 state. Importantly, the faster RISC processes of **O-D1** and **O-D2** than **C-D1** indicate the more effective conversion of triplet excitons into the singlet ones in the alkoxy-encapsulated dendrimers [42]. The photoluminescent quantum yield (PLQY) of the **O-D1** and **O-D2** doped films are 65% and 74% respectively, which is higher than that of **C-D1** film (53%), consistent with the slower non-radiative decay

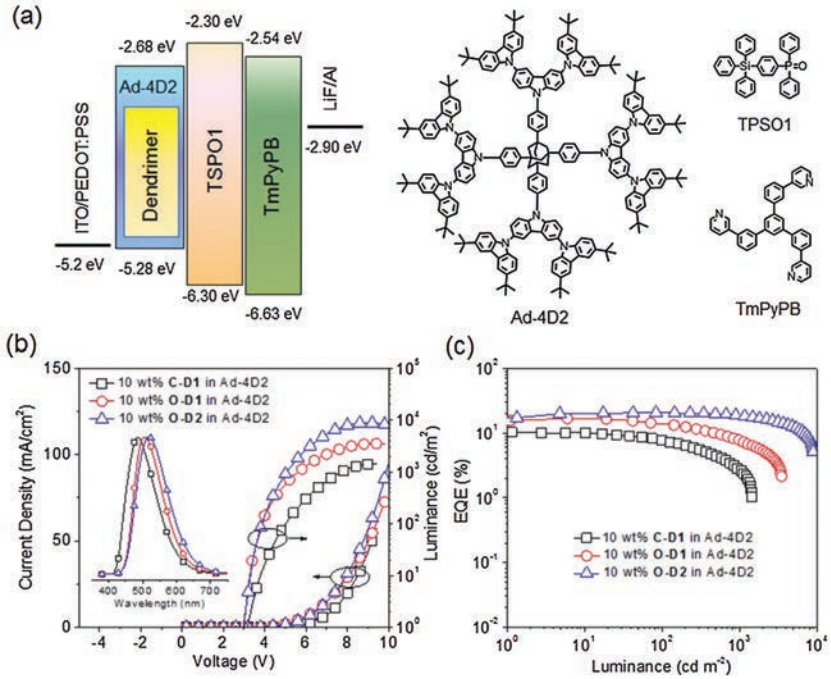

Fig. 4. Device configuration, energy levels and structures of the materials (a), current density-voltage-luminance (*J-V-L*) curves and EL spectra (b), and EQE-L curves (c) for devices with EML of 10 wt% dendrimers doped in Ad-4D2 host.

Table 2
Device performance of solution-processed OLEDs with EML of 10 wt% dendrimers doped in Ad-4D2.

Dendrimer	V_{on} (V)[a]	Maximum value/at 100 cd/m^2/at 1000 cd/m^2		L_{max} (cd/m^2)[d]	CIE(x, y)[e]
		LE (cd/A)[b]	EQE (%)[c]		
C-D1	3.2	24.9/18.6/6.3	10.1/7.7/2.8	1441	0.21, 0.35
O-D1	3.0	50.0/42.5/23.8	16.8/14.3/7.8	3525	0.26, 0.50
O-D2	3.0	63.3/63.0/56.1	20.6/20.5/18.2	8963	0.30, 0.52

[a] Turn-on voltage (at 1 cd/m^2).
[b] Luminous efficiency.
[c] External quantum efficiency.
[d] Maximum luminance.
[e] CIE coordinates.

and faster RISC processes (Table S1 in Supporting information) in the *n*-butoxy-substituted dendrimers.

To investigate the EL performance, two kinds of solution-processed OLEDs were fabricated with the configuration of ITO/PEDOT:PSS (poly(3,4-ethylenedioxythiophene):poly(styrene sulfonic acid), 30 nm)/Emissive layer (40 nm)/TSPO1 (diphenyl (4-(triphenylsilyl)phenyl)phosphine oxide [43], 8 nm)/TmPyPB (1,3,5-tri(m-pyrid-3-ylphenyl)benzene [44], 42 nm)/LiF(1 nm)/Al (100 nm). One is the non-doped devices using the dendrimer neat films as emissive layers (EML), the other is the doped devices with EMLs of dendrimers doped in the adamantane-cored dendritic host material Ad-4D2 at concentration of 5 wt% and 10 wt%. In both non-doped and doped devices, the dendrimers show typical EL spectra from the charge transfer emissions (Fig. 4b and Figs. S14 and S15 in Supporting information), with the emission peaks moving toward longer wavelength in the order of **C-D1**, **O-D1** and **O-D2**. The emission from the host is not observed in the doped devices, implying that the energy transfer from Ad-4D2 to the dendrimers is efficient in the EML.

The current density (*J*)–voltage (*V*)-luminance (*L*) characteristics, as well as the luminance dependence of external quantum efficiency (EQE) for the devices is shown in Figs. 4b and c and Figs. S14 and S15. The device performances are summarized in Table 2 and Table S1. The non-doped devices show maximum luminous efficiency (LE) of 2.2 cd/A, 10.4 cd/A and 24.3 cd/A as well as maximum EQEs of 1.6%, 3.2% and 7.9% for **C-D1**, **O-D1** and **O-D2**, respectively. In comparison, the doped devices show much higher device performance with the maximum LEs increased to 24.9 cd/A, 50.0 cd/A and 63.3 cd/A, corresponding to the maximum EQEs of 10.1%, 16.8% and 20.6% for **C-D1**, **O-D1** and **O-D2**, respectively. Compared to those for **C-D1**, efficiencies of both the doped and non-doped devices for **O-D1** and **O-D2** are greatly improved. Especially, for the 10 wt% doped devices, the maximum EQEs of **O-D1** and **O-D2** are ~1.6 and ~2.0 times that of **C-D1**. The enhanced device efficiency is reasonable considering that **O-D1** and **O-D2** exhibit much faster RISC process ($1.07 \times 10^{-6} \sim 1.67 \times 10^{-6}$ s^{-1}) than **C-D1** does (0.34×10^{-6} s^{-1}), leading to more effective utilization of triplet excitons in the devices. It is noted that the devices based on **O-D2** also show gentle efficiency roll-off. For example, EQE of the doped device containing 10 wt% **O-D2** can be kept at 20.5% at 100 cd/m^2 and 18.2% at 1000 cd/m^2, which is remarkable for TADF OLEDs through solution processes. The small efficiency roll-off can be attributed to the large size of 2nd-generation carbazoledendrons of **O-D2** which protect the emitting

core from unwanted intermolecular interactions, leading to inhibited triplet-triplet annihilation (TTA) and triplet-polaron annihilation (TPA) at high luminance.

In summary, we have demonstrated a new strategy for highly efficient TADF dendrimers by alkoxy encapsulation of the dendritic donor-acceptor emitters consisting of carbazoledendrons and triazine cores. Compared to the *tert*-butyl counterpart, the alkoxy encapsulating groups can reduce the singlet-triplet energy gap from 0.21 eV to 0.02 eV, which accelerates the RISC rate constant from 0.34×10^{-6} s^{-1} to 1.67×10^{-6} s^{-1}. Consequently, solution-processed OLEDs based on the dendrimers bearing alkoxy-encapsulated second-generation carbazoledendrons exhibit state-of-the-art device efficiency with the maximum EQE up to 20.6%. These results indicate that alkoxy encapsulation of the carbazole-based TADF dendrimers is a promising approach for developing highly efficient emitters for solution-processed OLEDs.

Declaration of competing interest

The authors declare that they have no known competing financial interests or personal relationships that could have appeared to influence the work reported in this paper.

Acknowledgments

We gratefully acknowledge the financial support from the Science and Technology Development Plan Project of Jilin Province (No. 20180520003JH), the Natural Science Fund Project of Changchun University of Science and Technology (No. XQNJJ-2017-14) and the Youth Innovation Promotion Association of Chinese Academy of Sciences (No. 2015180).

Appendix A. Supplementary data

Supplementary material related to this article can be found, in the online version, at doi:https://doi.org/10.1016/j.cclet.2020.06.025.

References

[1] A. Endo, K. Sato, K. Yoshimura, et al., Appl. Phys. Lett. 98 (2011) 083302.
[2] H. Uoyama, K. Goushi, K. Shizu, H. Nomura, C. Adachi, Nature 492 (2012) 234–238.
[3] Y. Liu, C. Li, Z. Ren, S. Yan, M.R. Bryce, Nat. Rev. Mater. 3 (2018) 18020.
[4] M.Y. Wong, E. Zysman-Colman, Adv. Mater. 29 (2017) 1605444.
[5] Y. Im, M. Kim, Y.J. Cho, et al., Chem. Mater. 29 (2017) 1946–1963.
[6] Y. Tao, K. Yuan, T. Chen, et al., Adv. Mater. 26 (2014) 7931–7958.
[7] Z. Yang, Z. Mao, Z. Xie, et al., Chem. Soc. Rev. 46 (2017) 915–1016.
[8] X. Cai, S.J. Su, Adv. Funct. Mater. 28 (2018) 1802558.
[9] T. Chatterjee, K.T. Wong, Adv. Opt. Mater. 7 (2019) 1800565.
[10] S.Y. Byeon, D.R. Lee, K.S. Yook, J.Y. Lee, Adv. Mater. 31 (2019) 1803714.
[11] T.T. Bui, F. Goubard, M. Ibrahim-Ouali, D. Gigmes, F. Dumur, Beilstein J. Org. Chem. 14 (2018) 282–308.
[12] T. Huang, W. Jiang, L. Duan, J. Mater. Chem. C 6 (2018) 5577–5596.
[13] Y. Zou, S. Gong, G. Xie, C. Yang, Adv. Opt. Mater. 6 (2018) 1800568.
[14] Y. Xie, Z. Li, J. Polym. Sci. A: Polym. Chem. 55 (2017) 575–584.
[15] Q. Wei, Z. Ge, B. Voit, Macromol. Rapid Commun. 40 (2019) 1800570.
[16] S.Y. Shao, J.Q. Ding, L.X. Wang, Chin. Chem. Lett. 27 (2016) 1201–1208.
[17] T.C. Jiang, Y.C. Liu, Z.J. Ren, S.K. Yan, Polym. Chem. 11 (2020) 1555–1571.
[18] A.E. Nikolaenko, M. Cass, F. Bourcet, D. Mohamad, M. Roberts, Adv. Mater. 27 (2015) 7236–7240.
[19] Y. Hu, W. Cai, L. Ying, et al., J. Mater. Chem. C 6 (2018) 2690–2695.
[20] S. Shao, J. Hu, X. Wang, et al., J. Am. Chem. Soc. 139 (2017) 17739–17742.
[21] X. Ban, Y. Liu, J. Pan, et al., ACS Appl. Mater. Interfaces 12 (2020) 1190–1200.
[22] M.K. Hung, K.W. Tsai, S. Sharma, J.Y. Wu, S.A. Chen, Angew. Chem. Int. Ed. 58 (2019) 11317–11323.
[23] C. Li, Y. Xu, Y. Liu, et al., Nano Energy 65 (2019) 104057.
[24] X. Wang, S. Wang, J. Lv, et al., Chem. Sci. 10 (2019) 2915–2923.
[25] J. Hu, Q. Li, X. Wang, et al., Angew. Chem. Int. Ed. 58 (2019) 8405–8409.
[26] C. Tang, T. Yang, X. Cao, et al., Adv. Opt. Mater. 3 (2015) 786–790.
[27] X. Li, K. Wang, Y.Z. Shi, et al., J. Mater. Chem. C 6 (2018) 9152–9157.
[28] J. Hu, X. Zhang, D. Zhang, et al., Dyes Pigm. 137 (2017) 480–489.
[29] D. Zhou, D. Liu, X. Gong, et al., ACS Appl. Mater. Interfaces 11 (2019) 24339–24348.
[30] D. Zhou, C.H. Ryoo, D. Liu, et al., Adv. Opt. Mater. 8 (2020) 1901021.
[31] S.C. Lo, P.L. Burn, Chem. Rev. 107 (2007) 1097–1116.
[32] X. Xu, X. Yang, J. Zhao, G. Zhou, W.Y. Wong, Asian J. Org. Chem. 4 (2015) 394–429.
[33] K. Albrecht, K. Matsuoka, K. Fujita, K. Yamamoto, Angew. Chem. Int. Ed. 54 (2015) 5677–5682.
[34] K. Albrecht, K. Matsuoka, D. Yokoyama, et al., Chem. Commun. 53 (2017) 2439–2442.
[35] K. Albrecht, K. Matsuoka, K. Fujita, K. Yamamoto, Mater. Chem. Front. 2 (2018) 1097–1103.
[36] Y. Li, G. Xie, S. Gong, K. Wu, C. Yang, Chem. Sci. 7 (2016) 5441–5447.
[37] X. Liao, X. Yang, R. Zhang, et al., J. Mater. Chem. C 5 (2017) 10001–10006.
[38] K. Sun, Y. Sun, W. Tian, et al., J. Mater. Chem. C 6 (2018) 43–49.
[39] J. Yoon, S. Choi, C.H. Jeong, et al., Dyes Pigm. 170 (2019) 107650.
[40] S. Shao, S. Wang, X. Xu, et al., Chem. Sci. 9 (2018) 8656–8664.
[41] Z. Ma, W. Dong, J. Hou, et al., J. Mater. Chem. C 7 (2019) 11845–11850.
[42] S. Wu, M. Aonuma, Q. Zhang, et al., J. Mater. Chem. C 2 (2014) 421–424.
[43] M. Mamada, S. Ergun, C. Perez-Bolivar, P. Anzenbacher Jr., Appl. Phys. Lett. 98 (2011)073305.
[44] S.J. Su, T. Chiba, T. Takeda, J. Kido, Adv. Mater. 20 (2008) 2125–2130.